Analysis of RF thrusters with TOPICA and a global system-level model

IEPC-2007-364

Presented at the 30th International Electric Propulsion Conference, Florence, Italy
September 17-20, 2007

Vito Lancellotti*, Giuseppe Vecchi, Riccardo Maggiora
Dipartimento di Elettronica, Politecnico di Torino, Torino, I-10129, Italy

Daniele Pavarin†, Simone Rocca‡
CISAS G. Colombo, Padova, I-35131 Italy

and

Cristina Bramanti§
Advanced Concepts Team, ESA-ESTEC, Noordwijk, The Netherlands

Abstract—Recent advances in plasma-based propulsion systems have led to the development of electromagnetic (RF) generation and acceleration systems, capable of providing highly controllable and wide-ranging exhaust velocities, and potentially enabling a wide range of missions from KWs to MWs levels. In this paper we report the results obtained by the development of TOPICA 3D code for modelling the RF antennas in space thrusters. TOPICA is a self-consistent code, which was originally conceived for plasma facing antennas operating in tokamaks, and recently extended to handle cylindrically symmetric plasmas. TOPICA has been validated by analyzing the ICRH unit of a three-stage helicon plasma thruster composed of a helicon plasma source, a confining magnetic field structure enclosing a plasma heating section, and a magnetic nozzle. The simulations are aimed at improving the penetration and coupling of the RF waves with the magnetized plasma in order to enhance plasma heating and axial thrust. The results of TOPICA has been used as input of a system-level modelling. This combination enabled to optimize the design parameters: antenna shape, generators, matching circuits, as well as the ensuing required power, mass and other physical quantities, including magnetic field for confinement. We have divided the study into two different and linked parts: 1) RF system modelling, which provides an "interface" between the RF power generation and the power deposition into the plasma and relies on the TOPICA code, and 2) plasma device modelling of the sub-systems and of their connection, which yields the global, system-level description of the engine).

*vito.lancellotti@polito.it
†daniele.pavarin@unipd.it
‡simone.rocca@onera.fr
§cristina.bramanti@esa.int

Nomenclature

$\mathbf{J}$	= electric surface current density [A/m]
$\mathbf{M}$	= magnetic surface current density [V/m]
$\tilde{\Upsilon}(m, k_z)$	= spectral tensor Green's function [1/Ω]
$[Y]$	= antenna admittance matrix [1/Ω]
R_c	= antenna loading resistance [Ω]
$n_{e,i}$	= electron, ion density [1/m^3]
Γ	= source or loss particle rate [particles/(s m^3)]
η	= thrust efficiency
P	= power [W]

I. Introduction

I.A. Background and motivations

PLASMA-BASED propulsion systems have found increasing interest in the past twenty years. Their conception and design derives directly from magnetic confinement fusion research, particularly of open magnetic "mirror" devices. Recent advances in plasma-based concepts have led to the identification of electromagnetic (RF) generation and acceleration systems as able to provide not only continuous thrust, but also highly controllable and wide-ranging exhaust velocities. This is of particular advantage in maneuvering applications such as planetary missions involving planetary orbit insertion/transfer and deep space cruise phases. Another key feature of RF-based plasma systems is their ability to produce energetic exhaust flows starting from light gases (H_2, D_2, He) giving very high specific impulse (up to 30,000 s) to heavier noble gases (Ar, Kr, Xe) with lower specific impulse but higher thrust. A side benefit of these RF-based designs is that they are electrodeless, with the related long device lifetimes, since sputtering problems due to ion impingement on grids are avoided. Furthermore, they are scalable from low-power (few kW) to high-power (>100 kW), thus making them suitable for a variety of mission applications. It is also to be stressed that these plasma thrusters have terrestrial applications in other sectors such as surface science, high-energy physics, and waste disposal.

The typical conceptual design of an RF plasma thruster is composed of an RF plasma source, an open-ended magnetic confinement device, an RF acceleration unit, and a "magnetic nozzle" (that might not be distinct from the confinement device). The plasma source comprises an RF driven helix-like antenna ("helicon") that energizes a flow of initially neutral gas, into magnetized plasma with high ionization fraction. The plasma outflow is confined into an elongated column by an intense magnetic field system, and then accelerated by a second RF driven device before exhaust flux through the "magnetic nozzle" structure of the magnetic field produced by the confinement coils near the acceleration region. The plasma source and the acceleration unit employ distinct RF systems and frequencies; the ubiquitous choice for the acceleration is to employ the Ion Cyclotron Resonance Heating (ICRH), a proven technology in fusion experiments for efficiently transferring large RF powers to magnetized plasmas, and exploited by the NASA VASIMR (VAriable Specific Impulse Magnetoplasmadynamic Rocket) propulsion system.[1,2] However, despite their distinct advantages in terms of performance of other forms of electric propulsion, some major challenges need to be overcome. These are primarily related to reducing the presently high specific mass and the large geometry of the system, as well as improving the thrust efficiency (at present the specific power is very high).

I.B. Objectives

In what follows we report on the development of a system-level modelling of a three-stage plasma thruster composed of a helicon plasma source, a confining magnetic field structure enclosing a plasma heating section, and terminating into a magnetic nozzle. This modelling can be employed to optimize the design parameters—say, antenna shape, matching circuits and generators, and the ensuing required power, mass and other physical quantities, including magnetic field for confinement—and to estimate its feasibility. In particular, our activity focuses on the most critical RF issues and on the RF-plasma interactions. To this purpose, the modelling has been divided into two different and linked parts: 1) RF system modelling (antenna and EM sources, Section II) and 2) modelling of the plasma device (i.e. sub-systems and relevant connections, Section

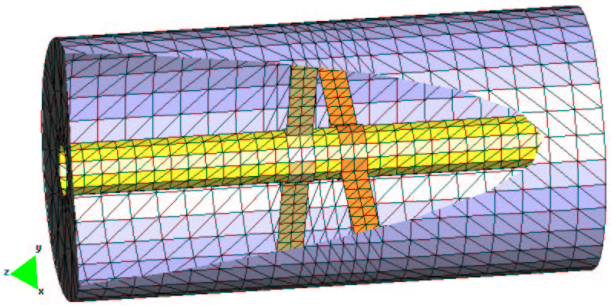

Figure 1. A CAD (electromagnetic) model of a sample ICRH unit including the thruster walls, a counter-driven two-loop antenna, and a cylindrical plasma flow: also shown is the 3D surface triangular-facet mesh for simulations with TOPICA.

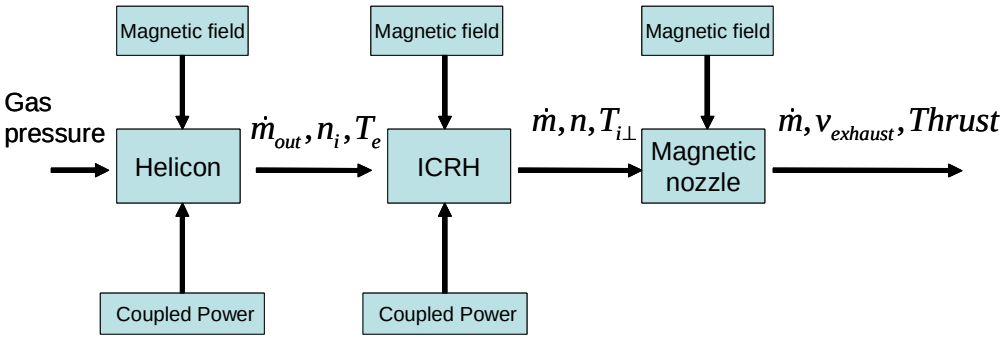

Figure 2. Block diagram of the zero-dimensional three-stage system-level model; input and output quantities to and from each component are indicated.

III). The former acts as an "interface" between the RF power generation and the power deposition into the plasma, whereas the latter provides the engine's global, system-level model.

As recalled above, the usual choice for the thruster acceleration unit is the ICRH, a well established technology in fusion experiments for transferring large RF powers to magnetized plasmas. To help design RF thruster ICRH antennas, TOPICA (Torino Polytechnic Ion Cyclotron Antenna) code, which was originally conceived for plasma facing antennas operating in tokamaks,[3] has been extended to handle cylindrically symmetric plasmas (see Fig. 1). The latter entailed developing a wholly new module of TOPICA charged with the task of solving Maxwell's equations in cylindrical magnetized warm plasmas and yielding the Green's function $\tilde{\Upsilon}(m, k_z)$, i.e. the relationship at the air-plasma interface between the transverse magnetic and electric fields in the spectral (Fourier) domain.

In addition, the approach to the problem of determining the antenna input admittance $[Y]$ relies on an integral-equation formulation for the self-consistent evaluation of the current distribution on the conductors. The simulations are aimed at improving the penetration and coupling of the RF waves with the magnetized plasma in order to enhance plasma heating and axial thrust.

Finally, a zero-dimensional electromagnetic model of the plasma device has been developed in order to provide an appreciation of its performance. As pictorially shown in Fig. 2, the model describes the three stages of the device, namely, plasma generation, heating and detachment. In the plasma generation section each species is followed in the electron impact reactions of ionization, dissociation, recombination, and excitation. In the heating stage the plasma absorbs the power emitted by the antenna ICRH, and in the magnetic nozzle the thermal energy of the plasma is converted into kinetic energy and the plasma is exhausted. This tool makes it possible to evaluate the required power, mass and other physical parameters, including magnetic field for confinement.

II. RF unit modelling with TOPICA

Basically, TOPICA's main purpose is to solve a set of integral equations (IE) for the self-consistent determination of suitable unknown electric ($\mathbf{J}$) and magnetic ($\mathbf{M}$) surface current densities, whence the

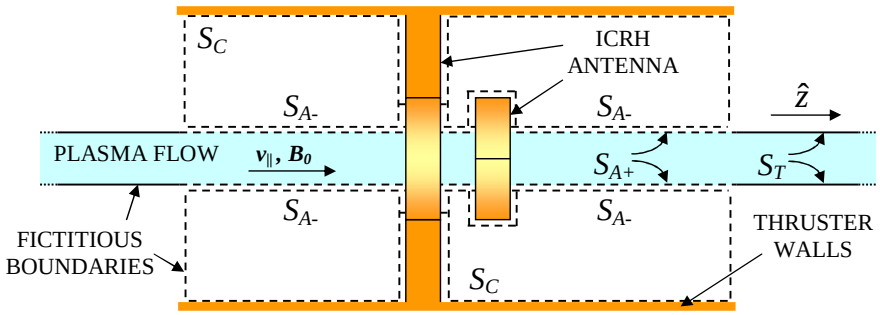

Figure 3. Cartoon of a typical ICRH unit featuring two loop antennas surrounding a plasma flow. Also sketched are the surfaces whereon the EP is applied and unknown surface current densities defined: in that regard, S_T needs neither be defined nor meshed, as the plasma Green's function already includes its effect.

admittance matrix $[Y]$ of an arbitrarily shaped antenna can be derived. Assuming the antenna has got N_P ports energized by as many coaxial lines, then $[Y]$ comes to be an N_P-order matrix.

In particular, the antenna of interest here is the one operating within the ICRH acceleration unit of an RF thruster and thus extending around a cylindrical plasma flow. A widely-used configuration for the RF booster consists of a counter-driven two-loop antenna encircling the plasma column, but we want to emphasize that the approach developed allows considering any shape of the antenna—and of the acceleration unit. On the contrary we do require the magnetically confined plasma to possess circular symmetry.

These assumptions are exemplified in Fig. 3, wherein a cross-sectional view of the structure under study is schematically depicted. According to Fig. 3, our acceleration unit model assumes the plasma faces the antennas—and all the other conducting bodies, for that matter—only through a cylindrical surface S_{A+} (dubbed *aperture* throughout) of finite extent, which is excised off an otherwise infinite metallic cylinder (S_T) coaxial to the plasma itself. As depicted in Fig. 3, the fictitious walls along with the aperture constitute a *cavity*—vaguely reminiscent of a drum with a median hole—wherein the antennas exist and radiate. The validity of our ICRH stage model can be backed as follows: for one thing, the whole structure size is usually several order in magnitude smaller than the vacuum wavelength, in view of the very low operating frequency (about 1 MHz is common), then we have the distance (h) between the cavity's side walls large enough as compared to the antenna size. Under those circumstances, we do expect h and the fictitious boundaries not to affect the antenna parameters significantly, although their sensitivity to h can be easily studied.

Due to the underlying formulation[3] of the electromagnetic problem, the plasma enters the equations only via its pertinent dyadic Green's function $\tilde{\Upsilon}(m, k_z)$ in the Fourier space, i.e. the rank-2 tensor linking the transverse-to-$\hat{\rho}$ magnetic and electric fields at the air-plasma interface ($\rho = a$):

$$-\tilde{\mathbf{H}}_t(a; m, k_z) \times \hat{\boldsymbol{\rho}} = \tilde{\Upsilon}(m, k_z) \cdot \tilde{\mathbf{E}}_t(a; m, k_z), \qquad \tilde{\Upsilon} = \tilde{\mathrm{Z}}^{-1} = \begin{bmatrix} \boldsymbol{Y_{\theta\theta}} & \boldsymbol{Y_{\theta z}} \\ \boldsymbol{Y_{z\theta}} & \boldsymbol{Y_{zz}} \end{bmatrix}, \tag{1}$$

with m (k_z) being the azimuthal (longitudinal) wavenumber. Therefore, a brand new module has been developed in charge of solving Maxwell's equations within a magnetized cylindrically-symmetric radially-inhomogeneous warm plasma and then yielding $\tilde{\Upsilon}(m, k_z)$. As per the plasma model, the high speed plasma flow, occurring in the RF thrusters, is assumed to rapidly and wholly absorb the ion cyclotron waves launched by the antennas;[4] moreover, the plasma velocity, which manifests its effect by shifting the ion cyclotron frequency,[6] is accounted for as well.

For these reasons and since no limitations at all are posed to the antenna shape, as already mentioned, the present version of TOPICA appears a substantive improvement of a previous more simplified approach.[7] Nonetheless, the electromagnetic problem shown in Fig. 3 is tackled exactly as described in an extensive work on TOPICA:[3] two coupled IEs can be stated, upon invoking the Equivalence Principle (EP)[8] twice and then enforcing the boundary and continuity conditions the tangential fields obey on S_C, $S_{A\pm}$. This two-step application of the EP yields two unknown surface current densities, $\mathbf{J}_C$ and $\mathbf{M}_{A-}$; the fields dependence on $\mathbf{J}_C$, $\mathbf{M}_{A-}$ is linear and represented by surface integrals with appropriate kernels (i.e. Green's functions).[9] To be specific, within the cavity we use the free space scalar Green's function, whereas on the plasma side (S_{A+}) we need to employ $\tilde{\Upsilon}$ given in (1).

The IEs are solved by applying the Moment Method,[10] both in spatial and spectral domain, the latter

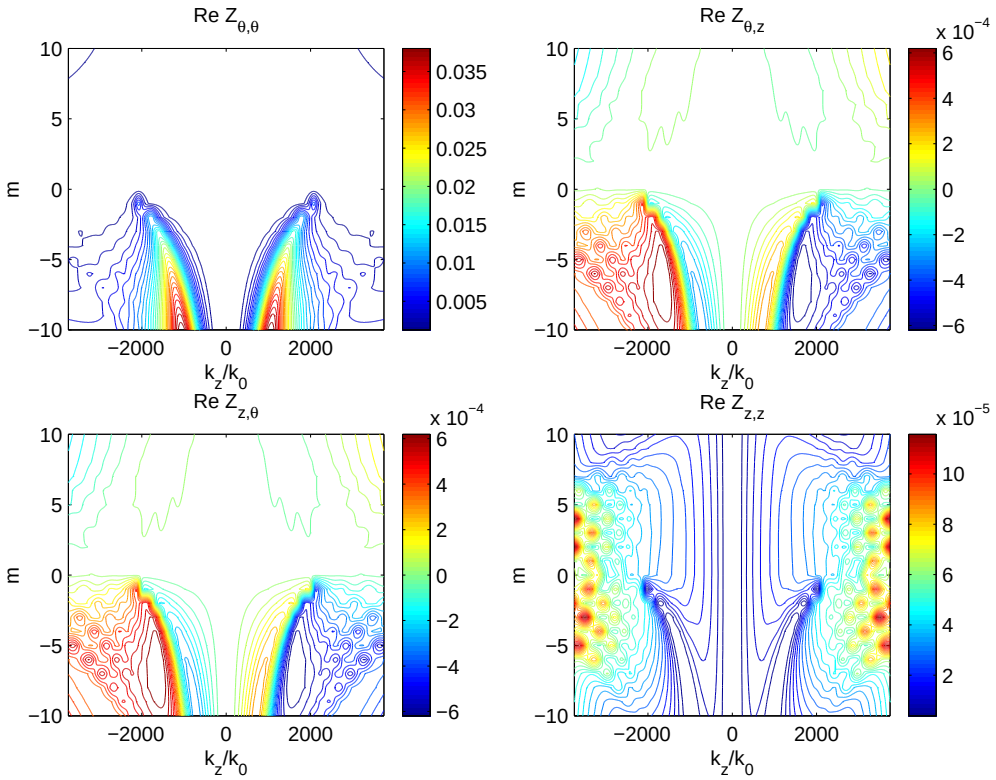

Figure 4. Real part of $\tilde{\mathrm{Z}}/Z_0$ entries as a function of m and k_z/k_0, with Z_0 (k_0) the free space impedance (wavenumber).

being the one wherein the plasma is more easily described. In particular, $\mathbf{J}_C$, $\mathbf{M}_{A-}$ are represented by a linear combination of a finite set of subdomain basis functions, which are defined over triangles (cf. Fig. 1). The coefficients of these linear combinations represent the actual unknowns of the problem, which is turned from a set of integral equations into an algebraic system.

III. Plasma device modelling

A numerical model describing the physics of the thruster is useful for a number of reasons: it permits to understand the physics of the mechanisms involved, it gives directions on the optimization and design of the experiment, it allows predicting the thruster performance, and it contributes to reduce the number of experiments required. The model resembles the three physical stages of the thruster: the plasma discharge, the RF plasma acceleration, and the magnetic nozzle. This section is aimed at providing a global time dependent model of a helicon source developed for producing plasma density above 10^{18} m^{-3}. The model combines a global plasma source simulation with a 0-dimensional gas-dynamic simulation and allows for changes in the neutral density, ionization, excitation and dissociation. The model outputs are: the density of each neutral and ionized specie, the electron density and temperature and the time history of each particle/energy loss channel.[11–13]

The plasma balance equations for particles and energy have been written to describe uniformly distributed plasma inside of a region determined by the magnetic field configuration. The neutral interaction with the plasma has been considered in this work by coupling a 0-dimensional gas-dynamic model of the entire system with a global plasma model of the source. The interactions taken into account in the model are:

- neutral density reduction due to ionization;
- neutral dissociation (molecular species-atom species);
- zero dimensional gas dynamic analysis behavior in the plasma source and in the vacuum chamber;
- wall recombination and volume recombination in the main vacuum chamber.

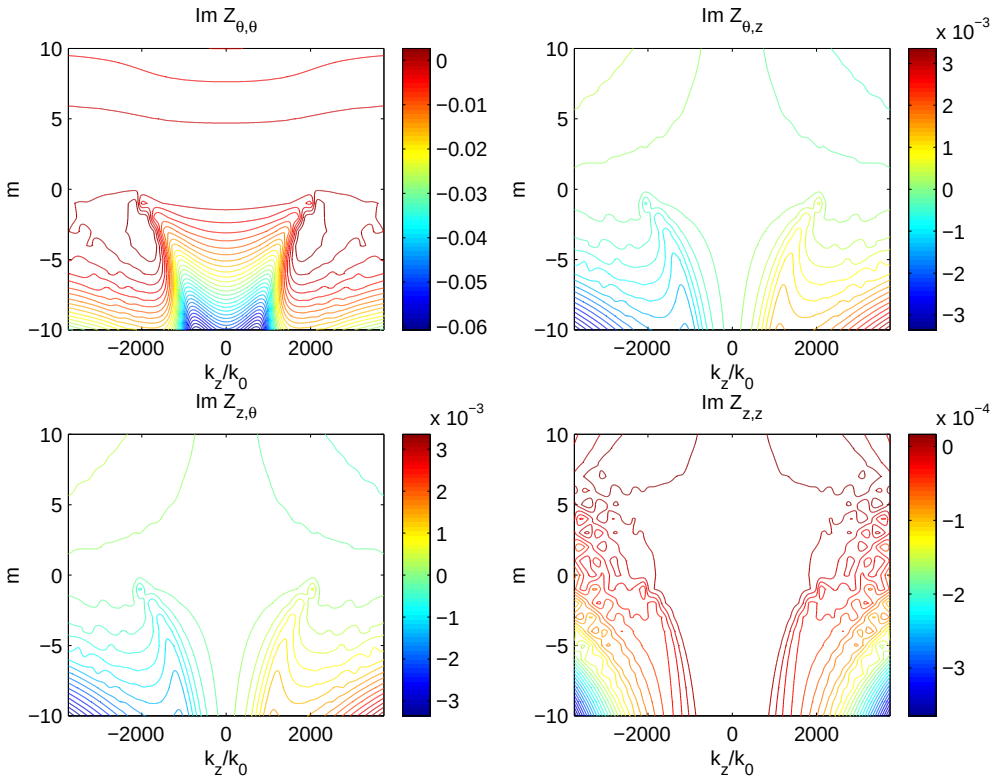

Figure 5. Imaginary part of $\tilde{Z}/Z_0$ entries as a function of m and k_z/k_0, with Z_0 (k_0) the free space impedance (wavenumber).

The particle balance equations for the ionized particles and electrons are written in a particle flux form, (particles/(s m^3). The general form for the balance equations of charged particles is:

$$\frac{dn_i}{dt} = \Gamma_i^s - \Gamma_i^l - \Gamma_{W,i} - \Gamma_{EXH,i}, \tag{2}$$

wherein Γ_i^s represents the source term due to plasma processes for the i-species, Γ_i^L is the loss term due to plasma processes, Γ_{Wi} is for the i-species the loss term due to particle recombination at the wall (the particle diffuses through the wall sheath before reaching the wall), and finally $\Gamma_{EXH,i}$ is the loss term due to the particle flow through the exhaust. The reaction rates were obtained averaging the cross section for the specific reaction over a maxwellian distribution:[14]

$$K_{iz} = \left(\frac{m}{2\pi k T_e}\right)^{3/2} \int_0^\infty \sigma(\nu)\nu \exp\left(-\frac{m\nu^2}{2kT}\right) 4\pi\nu^2 d\nu, \tag{3}$$

where T_e is the electron temperature in eV, and m is the electron mass, and σ the cross section. Wall losses are calculated as done in other works in literature.[11–13] Ions lost at the exhaust are computed as:

$$L_{EXH} = n_i u_B A_{EXH} \tag{4}$$

$$u_B = \sqrt{kT_e/m_i} \tag{5}$$

with u_B the ion Bohm's velocity and A_{EXH} is the geometrical exhaust area.

Another parameter affects the exhaust flow: in fact, at the exit of the plasma generation section the magnetic field increases and then decreases. This peak acts as a magnetic mirror that partly reflects the plasma flow. Therefore the net flow is given by the difference between the incident flow and the reflected flow. To calculate the electron temperature, the power balance equation has been written as follows (units W/m^3):

$$\frac{P_{ABS}}{V_e} = \frac{d}{dt}\left(\frac{3}{2} e n_e T_e\right) + P_W + P_{EXH} + \sum_i P_i, \tag{6}$$

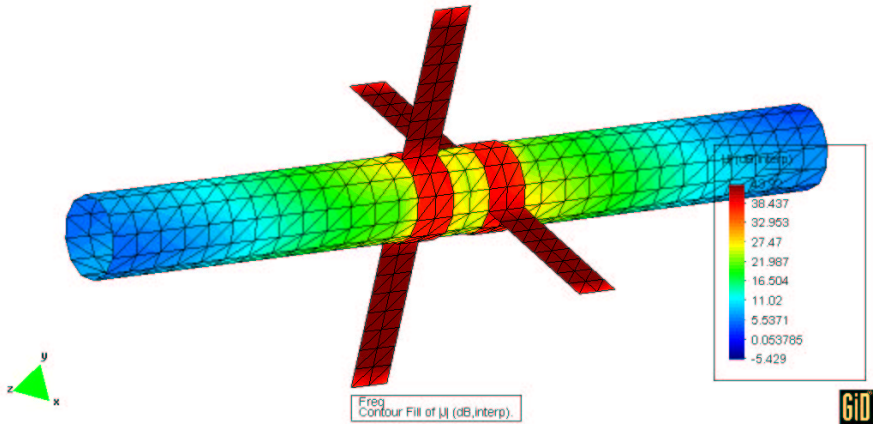

Figure 6. Standard counter-driven two-loop antenna: sample electric current magnitude distribution on conducting bodies and at plasma/air interface.

P_{ABS} is the deposited power into the plasma, which is assumed to be known, e is the electron charge, n_e the electron density, T_e is the electron temperature, V_e again the plasma volume, P_W is the power lost at the wall due to the electron-ions flow, P_{EXH} is the power loss associated with the electron and the ion flux at the exhaust, assuming that the escaping velocity is the ion-Bohm velocity. Eventually, the P_i terms constitute the power that is lost in the ith-reaction; their general expression is:

$$P_i = K_i E_{TH,i} n_e n_j, \tag{7}$$

where K_i is the rate constant for the specific reaction, E_{TH-i} the threshold energy for the ith-reaction,[15] n_j the density of the species involved in the ith-reaction. Experimental results[16] indicate the presence of a hot tail in the electron population in hydrogen and helium discharge. This distribution has been modelled summing two maxwellian distributions: one with the temperature of the bulk of the plasma and one with the temperature of the hot tail.

The ICRH is expected to heat the plasma to ion temperatures the order of 100 eV. Since the helicon heats the plasma to ion temperatures less than 1 eV, it seems reasonable to consider cold (T_i=0 eV) the plasma arriving at the ICRH. Therefore, it has been assumed that the plasma flow entering the ICRH region is monoenergetic with an axial velocity equal to u_2.

The power deposited by the ICRH is absorbed by the plasma in the form of normal kinetic energy:

$$\frac{1}{2} m v_{\perp 2}^2 = \frac{P_{ABS}}{n_2 u_2 A_2}. \tag{8}$$

Finally, downstream the ICRH, the magnetic nozzle converts part of the normal kinetic energy of the plasma into parallel kinetic energy, and thus produces thrust. This conversion is effective until the plasma detaches from the magnetic field lines. We assume that the detachment happens when the parallel kinetic energy density ($mnv_{||}^2/2$) becomes greater than the magnetic energy density ($B^2/2\mu_0$).

IV. Numerical results

The numerical approach outlined in Section II has been implemented in TOPICA, so that, once the current densities $\mathbf{J}_C$, $\mathbf{M}_{A-}$ have been computed, the antenna admittance matrix $[Y]$ along with other common parameters[3] can be obtained. The code has been thoroughly tested in vacuum, while preliminary results with plasma show good agreement with data available in literature.

To give an example of TOPICA's capabilities, we dealt with a neutral electron-helium ($^4He^+$) plasma and a two-loop ICRH antenna as in Fig. 1: listed in Table 1 are the main parameters involved in the simulation. The density profile has been assumed parabolic and given analytically, even though it may be read from file, if wanted.

A crucial intermediate step towards the solution is the calculation of the Green's function $\tilde{\Upsilon}(m, k_z)$, which accounts for all of the plasma effects. As mentioned in Section II, this is accomplished upon solving

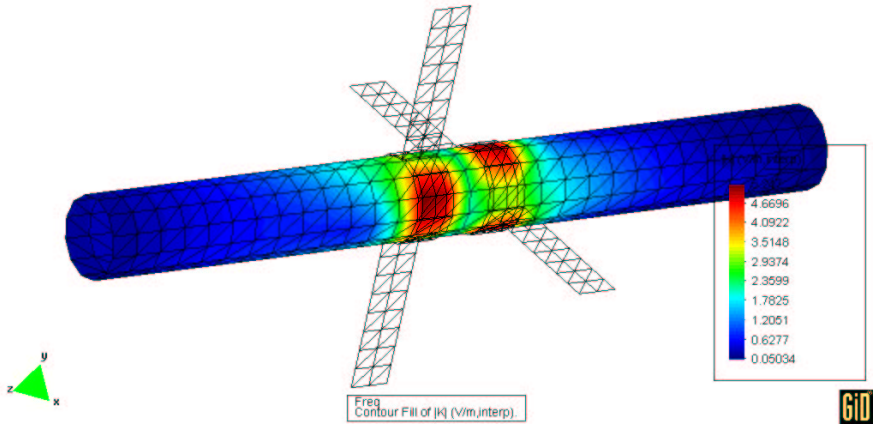

Figure 7. Standard counter-driven two-loop antenna: sample magnetic current magnitude distribution at plasma/air interface.

Table 1. Geometrical and physical data, single species ($^4He^+$) plasma

Loop radius (m)	0.021
Loop distance (m)	0.02
Plasma radius (m)	0.02
Density at center (m^{-3})	5.55 10^{19}
Density at edge (m^{-3})	0
Axial magnetic field (T)	0.25
Parallel velocity (m/s)	8 10^3
Ion perp./par. temp. (eV)	2
Electron perp./par. temp. (eV)	4

the Maxwell's equations within the plasma; the finite-element numerical scheme appears more stable if the magnetic field at the air-plasma interface is enforced and then the electric field is computed therein. In consequence, a tensor impedance $\tilde{\mathsf{Z}}$ being the natural output, $\tilde{\mathsf{Y}}(m, k_z)$ is obtained by inversion, in accordance with (1). Extensive numerical experiments have shown that, owing to the average size (the order of cm) of the triangular facets forming the aperture mesh, it suffices to compute $\tilde{\mathsf{Y}}(m, k_z)$ for m within the range from -60 to 60 (i.e. a grand total of 121 azimuthal modes) or even less, in order for the spectral integrals to converge.[3] For the sake of completeness, Fig. 4 and 5 show the real and imaginary part of the entries of $\tilde{\mathsf{Z}}$ germane to the case under study. The tensor is symmetric, as theory predicts, but each of the components lacks any symmetry along m, because of the confining magnetic field aligned with $\hat{\mathbf{z}}$—which is indeed suggestive of the non-reciprocal (gyrotropic) nature of the plasma.

We considered the standard counter-driven two-loop antenna shown in Figs. 6 and Fig. 7, wherein colors refer to the magnitude of the electric and magnetic surface current densities over the conducting bodies at the air-plasma interface, when the antenna terminals are driven by $\{+V, -V, +jV, -jV,\}$, respectively, since we want the whole antenna to launch an electric field with the circular polarization that maximizes the wave coupling to the $m = -1$ mode.[2] The electric current appears almost constant over the antenna loops, for the vacuum wavelength is pretty larger than the structure size. Besides, the magnetic current magnitude (that is the tangential electric field) is quite strong under the loops, which agrees with the expectation.

The main TOPICA's output is the antenna 4-by-4 admittance matrix $[Y]$, which in this instance may be further reduced to a 2-by-2 matrix, since each loop is driven with opposite voltages. The admittance matrix—or any other set of circuit parameters derivable therefrom—is the only quantity strictly required to carry out the design of the feeding and matching network and also to determine the radiated power P_{RF}. Apparently, the higher the power, the more efficient the antenna, but it is customary, however, to assess the ICRH antenna performance in terms of another figure of merit, namely, the coupling resistance

$$R_c = 2P_{\mathrm{RF}} / |I|^2, \tag{9}$$

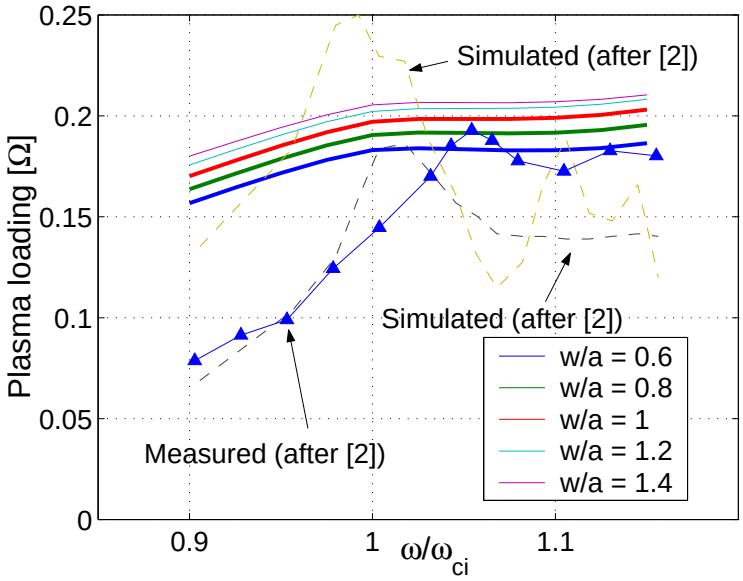

Figure 8. Standard counter-driven two-loop antenna: plasma loading as a function of the frequency computed with TOPICA for different loop-width to plasma-radius ratios. Also superimposed are measured data and simulations published in the work by Ilin.[2]

wherein I identifies the current entering the antenna terminals.

As an example, with the data reported in Table 1, we computed R_c for the loop antenna under investigation as a function of the frequency; results are plotted in Fig. 8, where the parameter of the curve is the ratio of the loop width to the plasma radius. For the sake of validation, the same graph also shows measured and simulated results published in the work by Ilin;[2] as can be seen the plasma loading predicted by TOPICA not only is well in the ballpark but also compares favorably with the measurements, and especially so at frequencies above the ion cyclotron resonance.

The global system-level model outlined in Section III and schematically exemplified in Fig. 2 has been implemented in a numerical suite as well. Although it can be run independently, the model reveals far more fruitful when it accepts as input, among others, the data from TOPICA, specifically the antenna radiated power. As a matter of fact this capability makes the overall approach self-consistent.

The typical results of the model are summarized in Fig. 9, which shows the thrust performance

$$\eta = \dot{m}v^2/(2P_{\mathrm{RF}}), \tag{10}$$

pertinent to a 10-kW thruster obtained through optimization by using the evolutionary algorithms. Analogous simulations made for input powers ranging from 1 kW to 100 kW gave results very similar to those shown. This means that the thruster's efficiency seems not to depend on the input power. The thrust performance increases with the specific impulse, basically because less power is needed to ionize the plasma and hence more power is diverted on the ICRH antenna that boosts the plasma.

Despite its simplicity, the lumped numerical model, however, yields a complete description of the physics of the thruster. This makes it possible to simulate the plasma behavior in the desired configuration and to determine the efficiency and thrust performance. The use of a finite-element model would have given more detailed and accurate results, but it would have required longer computational times, not compatible with the optimization process. The results of the model give the indication of the values of plasma parameters that should be expected during the experiment, and thus they give the requirements of the diagnostics needed. In particular the diagnostics should be able to measure plasma densities from 10^{17} m^{-3} to 10^{20} m^{-3} and electron temperatures up to 20 eV. The time evolution shows that the plasma probes should have a frequency pass-band from 0 to 1 kHz.

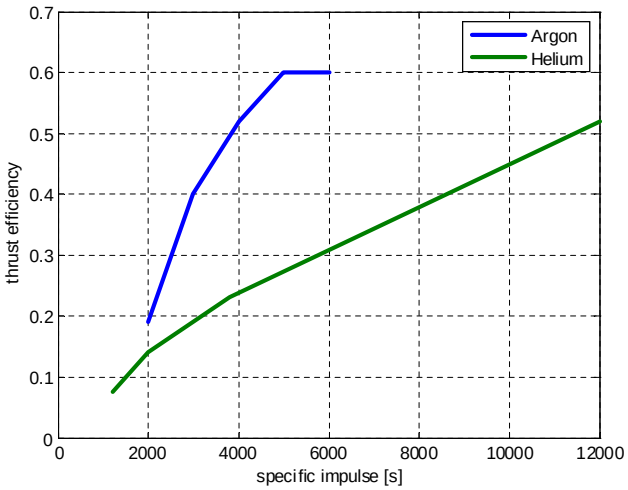

Figure 9. Thrust efficiency as a function of the specific impulse using helium and argon.

V. Conclusions

We have proposed a methodology to tackle the design of RF-based plasma thrusters. Our approach hinges on both TOPICA code and a plasma device zero-dimensional numerical model purposefully developed. The former stands out as a tool to accurately determine the ICRH antenna parameters (strictly related to the antenna shape and plasma composition) and the ensuing radiated power; the latter provides useful global system parameters, necessary to assess the engine performance. The coupling resistance predicted by TOPICA agrees well with available published data, and the same is true for the results from the thruster model (comparisons are not presented here). The developed tool can be used, for instance, to predict the feasibility of a low-power (a few kW) system and then address its scaling to high power. Therefrom, the resources required for the thruster physical realization can be finally estimated in terms of power, dimensions, mass and so forth.

Acknowledgements

This work was funded under the ARIADNA programme of the European Space Agency. The authors also gratefully acknowledge the valuable contribution of Dr Alessandro Cardinali with ENEA, Frascati (Italy), who helped them with the plasma tensor expression.

References

[1]J. P. Squire *et al.* 2003 *Fusion Science and Technology* **43** 111
[2]A. V. Ilin *et al.* 2004 *Proc. 42 AIAA*, No. 0151
[3]V. Lancellotti *et al.* 2006 *Nucl. Fusion* **46** S476
[4]E. Bearing, F. Chang-Diaz, J. Squire 2004 *The Radio Science Bulletin*, No. 310
[5]T. H. Stix 1992 *Waves in Plasmas*, (New York: American Institute of Physics)
[6]V. Ilin *et al.* 2005 *Proc. 43 AIAA*, No. 0949
[7]G. Vecchi *et al.* 2005 *16 Topical Conf. on RF Power in Plasmas,* AIP Conf. Proc., Vol. 787
[8]A. F. Peterson, S. L. Ray, R. Mittra 1998 *Computational Methods for Electromagnetics* (New York: IEEE Press)
[9]L. B. Felsen, N. Marcuvitz 1973 *Radiation and Scattering of Waves* (Englewood Cliffs: Prentice Hall)
[10]R. Harrington 1993 *Field Computation by Moment Methods* (New York: Oxford)
[11]Suwon C. 1996 *Physics of plasmas* **6**, 359-365.
[12]Zorat R. 2000 *Plasma Sources Sci. Tech.* **9** 161-168
[13]Lee C. 1995 *J. Vac. Sci. Tech. A* **13** (2) .
[14]M. A. Lieberman 1994 *Principles of Plasma Discharges and Material Processing* (New York: Wiley)
[15]R. K. Janev 1987 *Elementary processing hydrogen helium plasmas* (Springer-Verlag)
[16]M. I. Panevsky 2003 *Characterization of the Resonant Electromagnetic Mode in Helicon Discharges*, PhD Thesis, University of Texas at Austin